Disclaimer

This note has not been internally reviewed by the DØ Collaboration. Results or plots contained in this note were only intended for internal documentation by the authors of the note and they are not approved as scientific results by either the authors or the DØ Collaboration. All approved scientific results of the DØ Collaboration have been published as internally reviewed Conference Notes or in peer reviewed journals.

Summing Resistors for Central Calorimetry

D0 Note 1084

February 13, 1991

Maris Abolins, Dan Edmunds and Bo Pi
Michigan State University

Introduction

This note summarizes the results of work that led to the choice of trigger summing resistors for the Central Calorimeter (CC) module for the D0 detector.

Statement of Problem

Detector Overview

The CC calorimeter in D0 is constructed of 32 separate electromagnetic (EM) modules and 16 hadronic (HD), arranged in concentric cylinders around the beam axis covering approximately $\pm$ 1.2 units of pseudo-rapidity (η). The modules are further subdivided in azimuth giving 64 separate elements. In depth they consist of 4 layers of EM detectors, the third of which is partitioned laterally in 4 separate pieces, giving a total of 7 EM sections, followed by 4 layers of HD detectors, 3 fine hadronic (FH) and one coarse hadronic (CH) section. There are two kinds of trigger towers: the EM and the HD. Each is constructed of sums in depth over their respective sections (EM or HD) and a sum laterally over two units of η and ϕ, yielding 0.2x0.2 for the trigger tower granularity in $\Delta\eta$ x $\Delta\phi$. The depth sums for the EM section cover all seven sections of the EM towers but the HD include only the 3 FH layers. In the narrative to follow reference is frequently made to trigger towers by their η and ϕ indices[1]. The former range from 1 to 6 with each one referring to increasing $\Delta\eta$ values i.e. 0.0 to 0.2, 0.2 to 0.4 etc. Likewise the ϕ co-ordinate refers to successive trigger towers each covering a fraction $2\pi/32$ of the full azimuth. The co-ordinate system used is the D0 standard where z is positive along the proton direction, y is up and x is chosen to complete the right handed co-ordinate system. The ϕ co-ordinate starts at the x-axis and increases in the direction of the y-axis in the x-y plane. When reference is made to the readout towers comprising a trigger tower, the numbers 1 and 2 are used to represent increasing η and ϕ values within a given trigger tower.

Figure 1a is a schematic view of the calorimeter electronics showing a calorimeter cell with capacitance C_d attached to a pre-amplifier with feed back capacitor C_{fb}. The trigger pickoff is followed by two stages of summing, the first sums in depth and laterally over ϕ while the second adds the two pieces in η. The gain of each stage is set by the respective ratio of the feedback resistors (3 KΩ) to the summing resistors. After summation, a line driver carries the signal to the line receiver circuitry shown in Figure 1b, which is located on the calorimeter trigger front end cards residing in the Trigger Framework in the moving counting house. Below we discuss the items in Figures 1a and 1b in more detail.

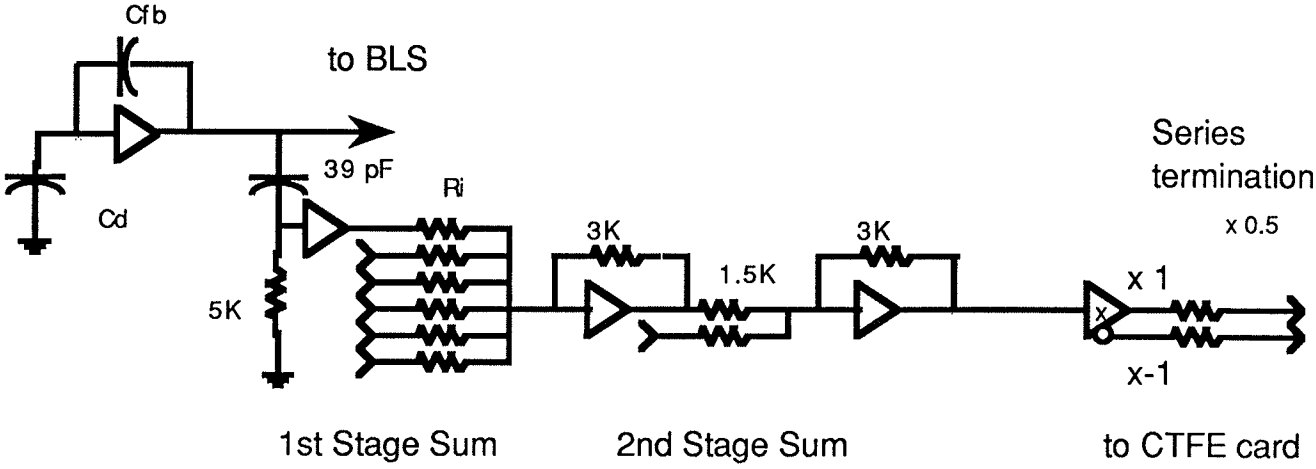

Figure 1a

[1] These indices find clear exposition in D0 Note 706.

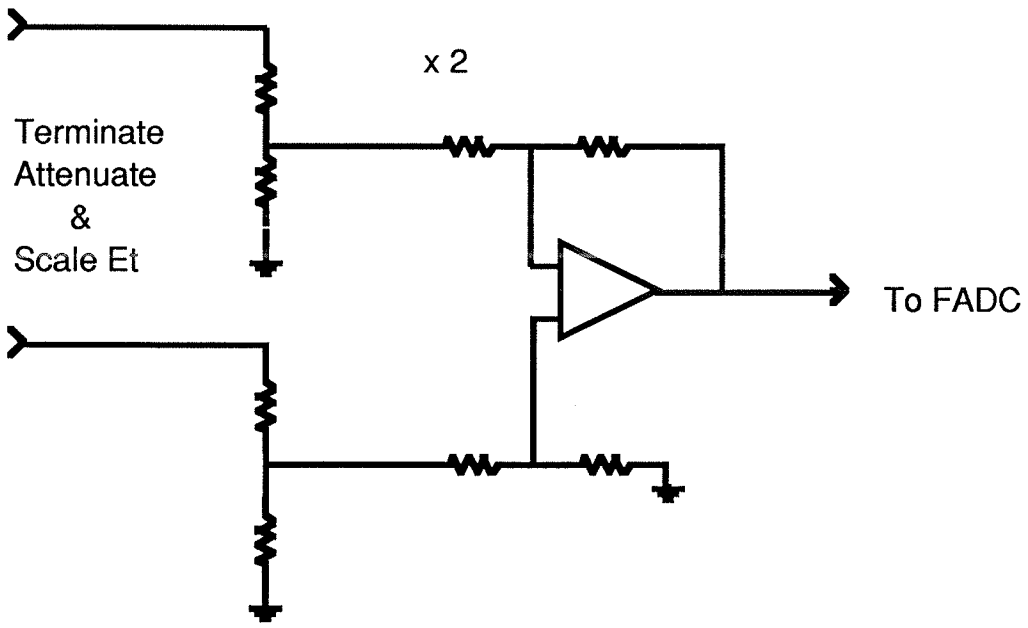

Figure 1b

Choice of parameters

Constants

An essential element in our considerations is the desire to set a maximum scale in E_t (- E sinΘ) to 64 GeV in a single channel and to have that transverse energy result in a 2 V signal swing at the input to the flash ADC on the Calorimeter Trigger Front End (CTFE) card. We note also the following useful constants:

$$e - 1.6 \times 10^{-19} \text{ Coulombs} \qquad (1)$$

N_{eG} - electrons/GeV energy deposited in liquid argon - 9.45×10^{6} (2)

Sampling Fractions & Feedback Capacitors

The sampling fractions relevant to the various detector sections are computed by taking the ratio of energy loss in the active (liquid argon) medium to the total energy loss in the module. The specific energy loss values for the materials in the detector were taken from the latest edition of the LBL wallet card.

The feedback capacitors, C_{fb} in Figure 1a, determine the voltage at the output of the preamplifier for given charge on the capacitor C_d. Their choices along with the relevant sampling fractions for the different detector pieces are summarized in Table I.

Table I

Sampling Fractions & Feedback Capacitors

Detector Section	Sampling Fraction (%)	Feedback Cap. (pF)
EM - 1	7.0[2]	5.5
EM - 2	12.7	5.5
EM - 3 (all sections)	12.7	10.5
EM - 4	12.7	10.5
FH - 1	7.0	5.5
FH - 2	7.0	5.5
FH - 3	7.0	5.5
CH	1.57	5.5

Note that CH, the coarse hadronic section is included only for completeness and is not used in constructing trigger sums.

Circuit calculations

Pre-amp output

Referring to Fig. 1a, the voltage at the output of an ideal pre-amp when an energy E (in GeV) is deposited in a calorimeter section is:

$$V_{pre-amp} = \frac{e \times N_{eG} \times E \times SF}{C_{fb}} \qquad (3)$$

where SF refers to the sampling fraction and C_{fb} the feedback capacitor.

Trigger pick-off gain

Referring once again to Fig. 1a, we see that the trigger signal is formed by differentiating the output of the pre-amp. The resulting amplitude depends on a number of circuit parameters among them the (cell plus cable) capacitance, C_d, the feed back capacitance, C_{fb} and the cable inductance, L. We have studied these effects in a number of ways: by simulating the circuit via SPICE, by making measurements on a test setup in the laboratory and by looking at the relative energy response of a trigger cell and the normal calorimeter readout in the test beam. We have achieved essential agreement of all three methods at the level of about 5%. Our studies indicate that the amplitude has a strong dependence on C_d, with C_{fb} and L representing corrections at the 10 - 20% level. The cables in CC vary in length from 11.7 to 25.8 feet with an average of 18.75 feet. To make the inductance corrections, we have found it sufficient to divide them into two sets, those with lengths nearer to 15 feet and those nearer to 22 feet and then use SPICE generated curves at

---

[2]We get 11.7% for this sampling fraction if we do not count the material in the cryostat walls. If this material (1/4" & 3/8" of stainless) is counted, the sampling fraction becomes 5.5%. According to actual measurements in the test beam (private communication from Tony Spadafora) the sampling fraction that optimizes resolution is in between the two values. We arbitrarily pick our sampling fraction to be 7%.

those discrete cable lengths as corrections for the two sets. Including the two values of the feedback capacitance we have four separate functions $G(C_d,C_{fb},L)$ to consider. These are shown in Figure 2[3].

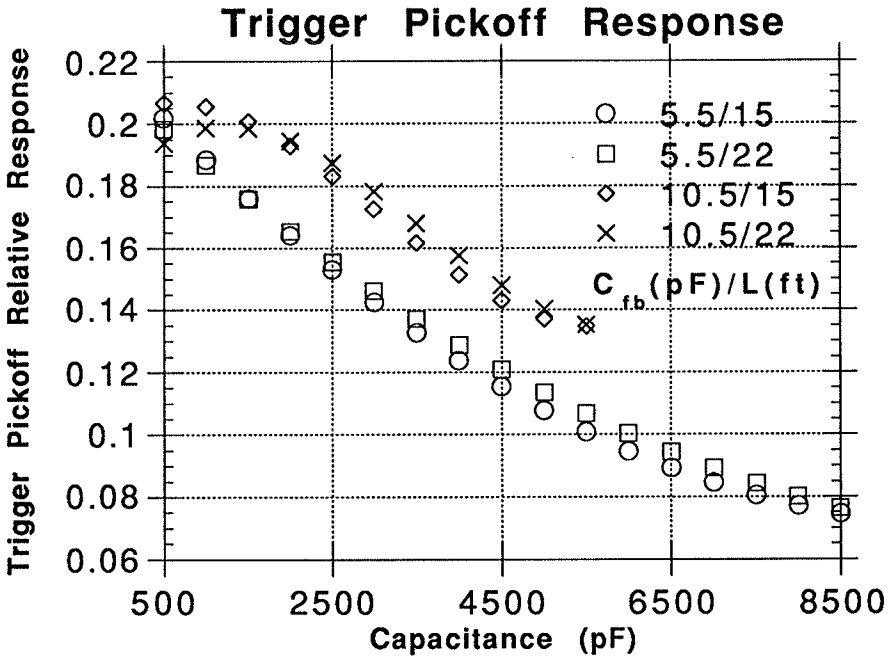

Figure 2

Gain of summing circuitry

A trigger tower is made by adding a number of trigger pick-offs in two stages, first in depth and over two values of ϕ at fixed η and then over the two η's[4]. The contribution of each amplitude to the sum is in proportion to R_{fb}/R_i where R_{fb} is the feedback resistor (3 kΩ) and R_i the series resistor. This is the expectation for an ideal circuit where the open loop

---

[3]The simulation put 1.322 GeV (1.322*10.5/5.5 GeV) of energy into the liquid argon (1.322/SF into the calorimeter) viewed by an amplifier with feedback capacitance 5.5 pF (10.5pF) with the gain of the first depth summer set at 3.0 and that of the second at 1.0. Two sets of curves were calculated, for C_{fb}-5.5 pF and 10.5 pF. The coefficients for the polynomials, with the capacitances expressed in units of nF, are given in the table below:

Polynomial coefficients

L(ft)	C_{fb}(pF)	x^0	x^1	x^2	x^3
15	5.5	0.4709	-0.062743	0.0031144	0
22	5.5	0.45873	-0.053502	0.002249	0
15	10.5	0.44293	0.027287	-0.02449	0.0026551
22	10.5	0.39937	0.061176	-0.029962	0.002796

[4]In a normal trigger tower this results in adding 7 x 2 = 14 channels for EM at stage 1 and 3 x 2 = 6 channels for HD. At stage 2 only two quantities are added in either case.

gain is very large. Actual measurements show that our circuit is not ideal, showing a dependence on the parallel resistance indicated in Figure 3[5].

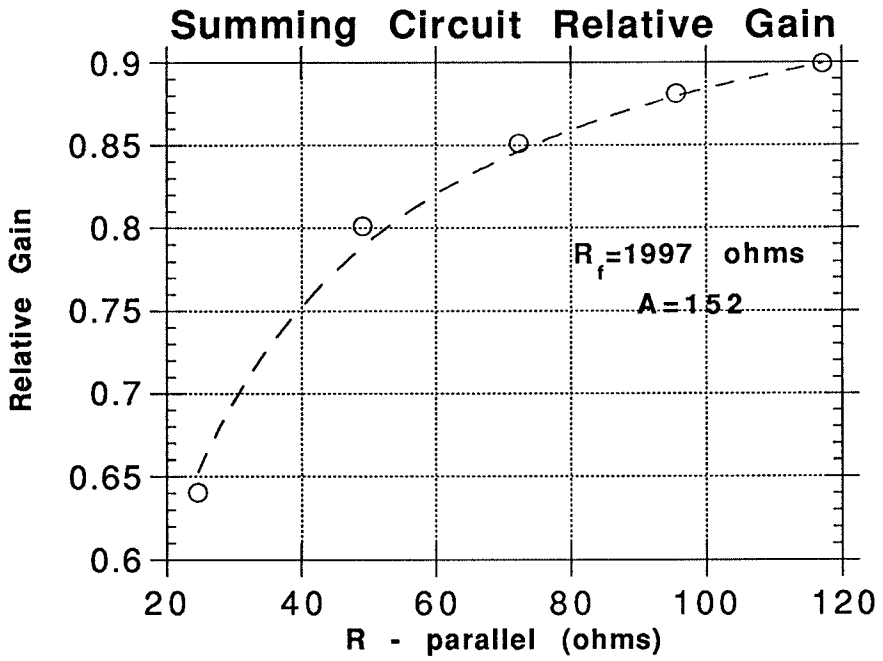

Figure 3

Here R_f is the series resistance and the gain, relative to the ideal, is plotted as a function of the total parallel resistance. The curve is from a fit to the form:

$$\frac{1}{(1+\frac{R_f}{A \cdot R_{par}})} \qquad (4)$$

where A is the open loop gain of the amplifier. If the resistors are all of comparable value then the dependence on them drops out and we get a "universal" curve that is a function of R_{par} only. Figure 4 shows all the measurements along with a single parameter fit which represents the data well. Henceforth, we shall refer to this "universal" curve as $H(R_{par})$

$$H(R_{par}) = \frac{1}{1+\frac{c}{R_{par}}}; c = 13.2 \qquad (5)$$

[5]The measurements of the behavior of the summing circuitry were performed by George Krafczyk.

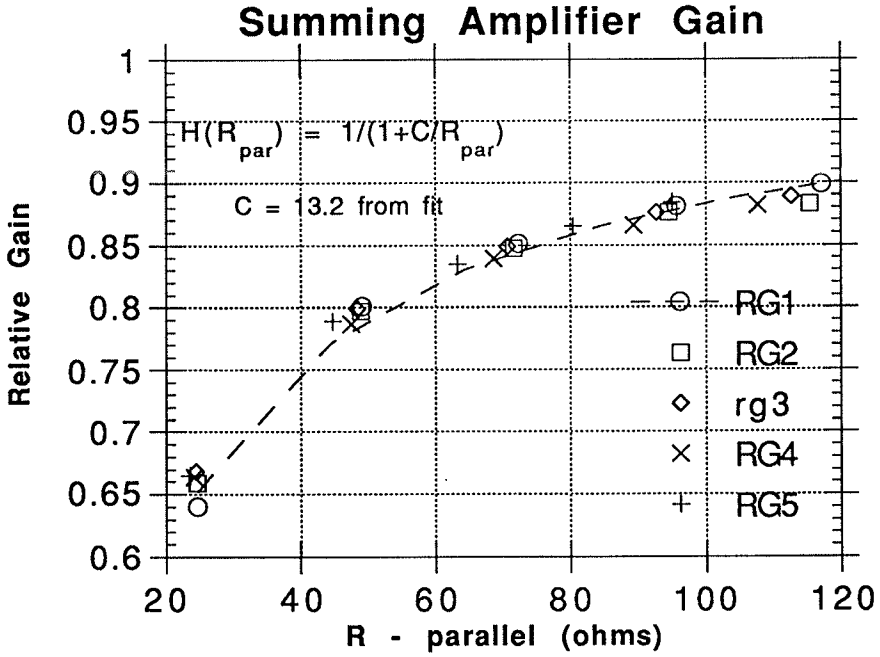

Figure 4

Choice of Resistors

Circuit considerations

Referring to Figure 1a we can now write down an expression for the voltage at the output of the first summing stage when energy E is deposited in the calorimeter:

$$V_{sum1} = V_{pre-amp} \cdot G(C_d, C_{fb}, L) \frac{3k\Omega}{R_{i1}} H(R1_{par}) \qquad (6)$$

The voltage at the output of the second summing stage is then similarly:

$$V_{sum2} = V_{sum1} \frac{3k\Omega}{R_{i2}} H(R2_{par}) \qquad (7)$$

This is also the value of the differential voltage appearing on the cable connecting the BLS and CTFE cards as the cables are terminated in series and at the far end.

The voltage applied to the FADC on the CTFE card is this differential voltage, multiplied by the gain of the termination attenuation network and the gain of the receiver circuit (fixed at 2). The gain of the termination attenuation network is adjusted to scale E (energy) to E_t (transverse energy) and is set to be 0.5 at 90°. Therefore, if we think in terms of transverse energy deposited in the calorimeter then the voltage into the FADC for fixed E_t deposit is independent of η and the gain of the receiver circuit equals unity.

Procedure

We proceed by assuming ideal response of the summing circuitry ($H(R_{par}) - 1$) and calculate values for the resistors, R_i, that generate a signal of 2 V at the input to the FADC's when 64 GeV of E_t is deposited in the calorimeter:

$$2V = \frac{e \cdot N_{eG} \cdot 64 \cdot SF}{C_{fb}} G(C_d, C_{fb}, L) \frac{3K\Omega}{R_i} \cdot \frac{3K\Omega}{1.5K\Omega} \qquad (8)$$

This expression may be solved for the resistor values R_i:

$$R_i = 290{,}304 \cdot \frac{SF}{C_{fb}} \cdot G(C_d, C_{fb}, L) \qquad (9)$$

where we have inserted the appropriate numerical constants. The resulting value is given in ohms if C_{fb} is expressed in pico-Farads.

Once the R_i at summing stage 1 are determined, we may calculate their parallel resistance, R_{par}. The attenuation at stage 1, $H(R_{par1})$ may be compensated at stage 2 to a good approximation by choosing:

$$R_{i2} = \frac{1{,}500}{(1 + \frac{C}{R_{par1}})} ohms \qquad (10)$$

Since R_{par1} is usually 50 Ω or more and C is about 13, R_{i2} will be around 1,200 Ω. The second stage of summing only has two inputs resulting in a total parallel input resistance of approximately 600 Ω. Therefore, the amplitude correction for the second summing stage can be completely ignored.

Capacitance Distribution

Our choice of resistors is determined by the values of the capacitances of individual detector elements and their associated cables. These values are derived from a combination of actual measurements and calculations and are summarized below in a number of graphs.[6]

---

[6]The values represent cold measurements of the actual cells at BNL added to calculated cable capacitances compensated for temperature change. I am grateful to Mr. Jaehoon Yu for supplying this information.

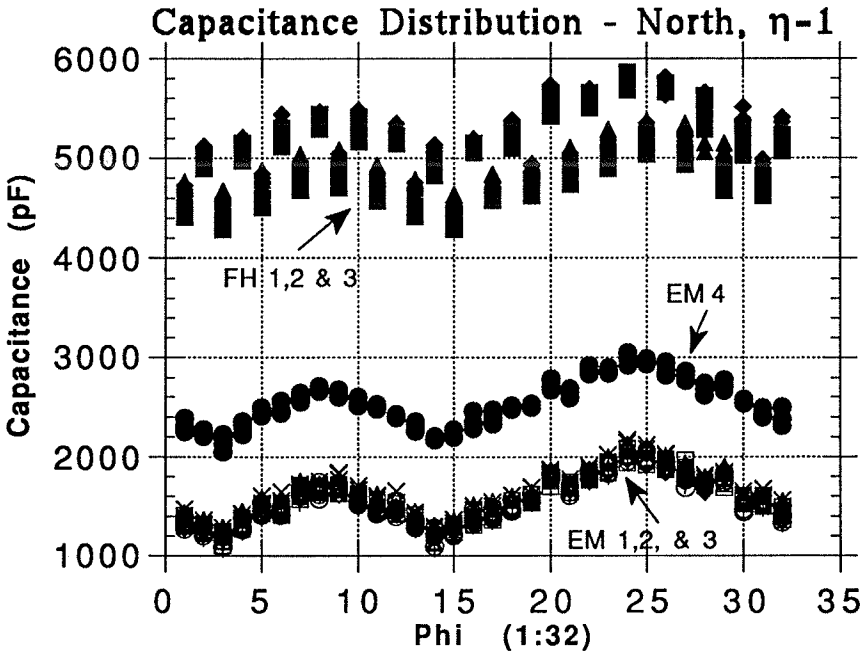

Figure 5

Figure 5 shows the distribution of capacitances for trigger tower η - 1, for all depths as a function of ϕ. Note the cable-induced azimuthal variation, the tight clustering of EM layers 1,2 & 3, the slightly increased capacitance in EM 4 and the odd-even effect in the FH modules. This same pattern is followed in Figures 6a and 6b, the analogous plots for trigger η towers 2 and 3, covering η's from 0.2 to 0.4 and 0.4 to 0.6 respectively.

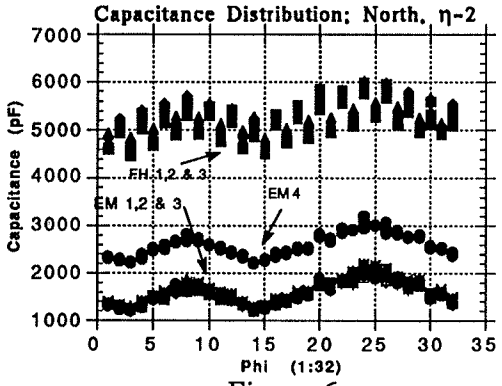

Figure 6a

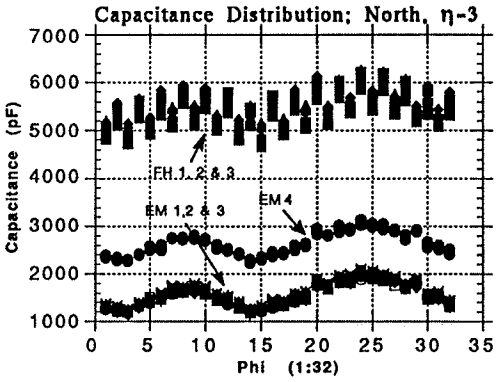

Figure 6b

In Figures 7a and 7b we start to see the effect of the edge of the CC modules resulting in progressively decreasing capacitance with η. The effect is seen first in FH 3 and then progressively in other layers of FH and EM.

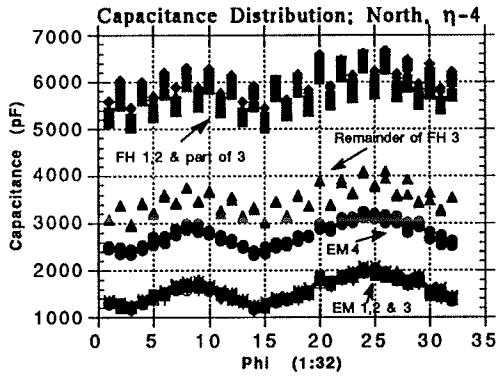

Figure 7a

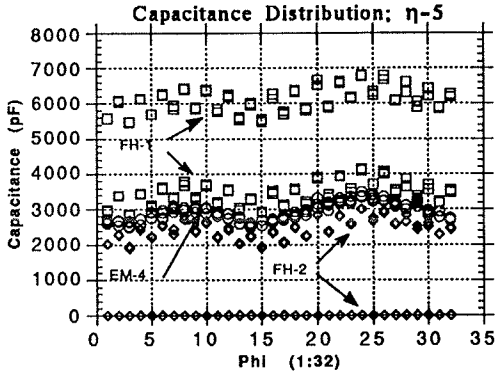

Figure 7b

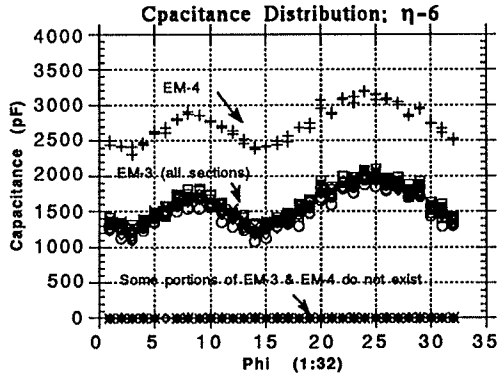

Figure 7c

Finally in Figure 7c we see the total disappearance of pieces of the calorimeter due to the geometrical cut-off effects.

All of the plots involving capacitances were for the North half of CC only. It is important to examine to what extent the North-South symmetry of the calorimeter is broken. This we proceed to do next.

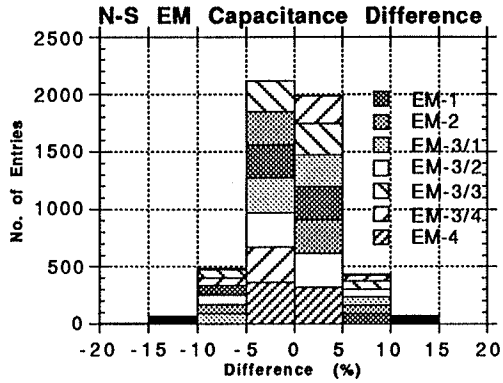

Figure 8a

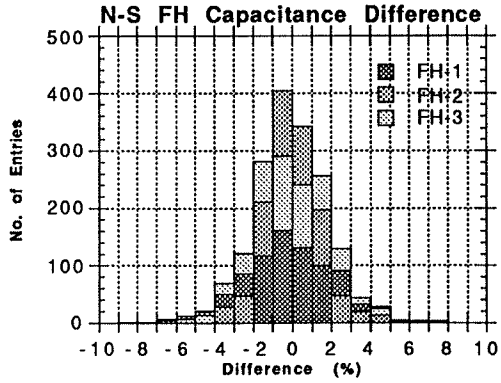

Figure 8b

Figures 8a and 8b show the percentage differences (N - S)/(N + S) of the EM and FH capacitances respectively. The distributions have widths of a few percent and insignificant tails. We shall see that differences at this level are not important.

We next examine the distribution of the capacitances in the pseudorapidity variable η at a fixed value of ϕ. In Figures 9a through 9d we see the η dependence of each of the four separate readout towers comprising an EM trigger tower. We note the smooth behavior of all sections of EM calorimetry for the η-1, ϕ-1,2 trigger tower subsections (Fig's. 9a and

9b) and the contrasting behavior of the η-2, ϕ-1,2 sections (Fig's. 9c and 9d) where the EM 4 sections and the higher η subsections of the subdivided EM 3 sections disappear.

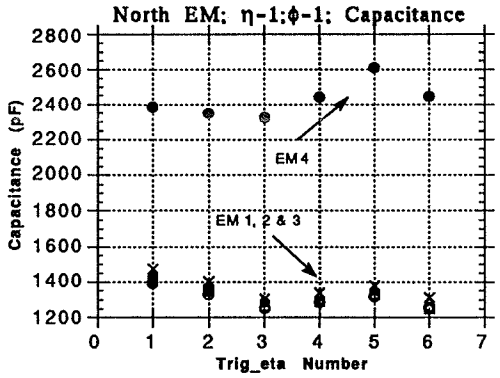

Figure 9a

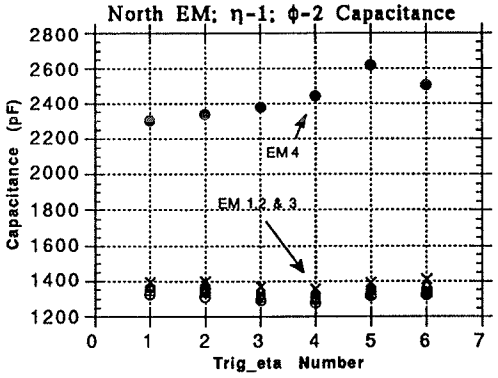

Figure 9b

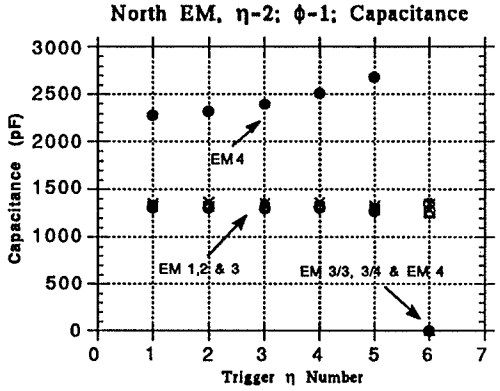

Figure 9c

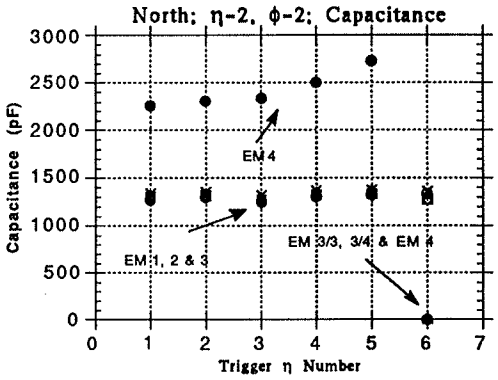

Figure 9d

Figures 10a, 10 b and 10c show the η dependence of FH1, FH2 and FH3 respectively with all four readout sections plotted together. One should note the modest rise of the capacitance with η and the sudden decrease near the module edge as the plates get smaller and finally disappear.

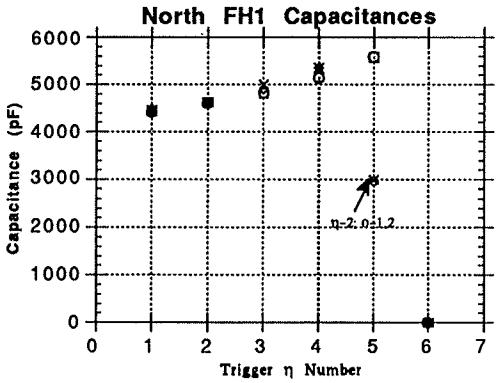

Figure 10a

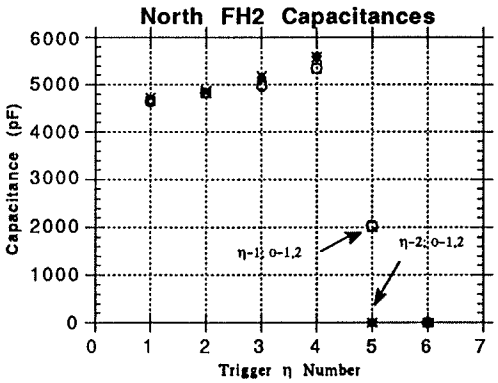

Figure 10b

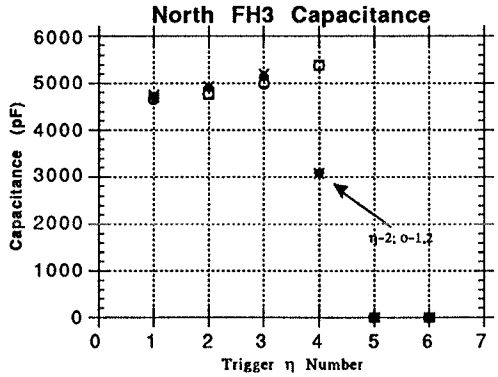

Figure 10c

Note that for FH3 the η-2, ϕ-1,2 plates get smaller for trigger η - 4 and that for trigger η-5 or 6, the elements no longer exist.

First Summing Stage

Method of Choice

Using Equation (9) we can readily calculate a resistance value for every cell in the calorimeter. The distribution of some of the resulting resistances is given in the plots below, first for some representative EM channels:

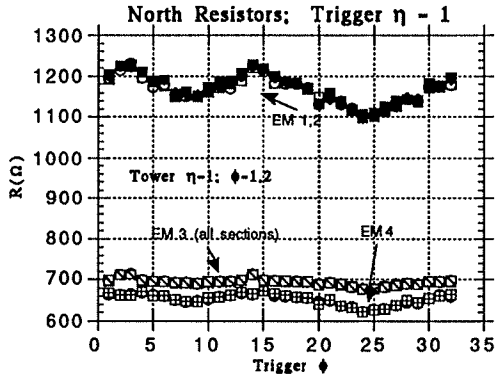

Figure 11a

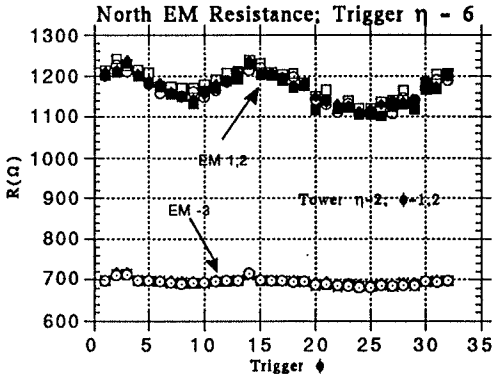

Figure 11b

and then some hadronic channels:

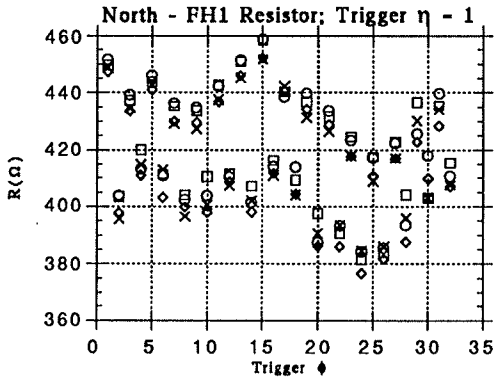

Figure 11d

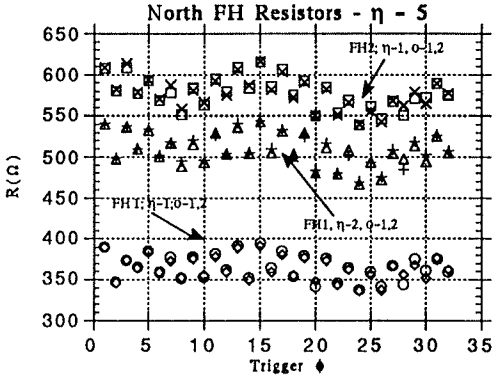

Figure 11e

We note that the resistance distribution is essentially a mirror image of the capacitance distribution. The effect of the decreased capacitance at the extreme ends of the detector is to lead to increased resistance values as the need for compensation is less.

In the interest of simplicity we wish to keep the number of different BLS cards as small as possible. This will involve some compromises involving the achievable resolution and we must examine these. We will choose the minimum number of possible BLS cards. The following assumptions govern our choice:

1) North - South symmetry is assumed.
2) Symmetry in azimuth (ϕ) is assumed.
3) There will be η symmetry until extreme elements of the detector change capacitance dramatically or disappear.

These assumptions lead to the following 4 sets of BLS cards with their respective η coverage ranges:

Set Number	η Range
1	0.0 - 0.6
2	0.6 - 0.8
3	0.8 - 1.0
4	1.0 - 1.2

For each set we compute the average values of the required resistors at each summing position and then rationalize them to the nearest available 1% resistors[7]. To measure the effect of these choices on our resolutions we next compute the fractional deviations of the individual channel resistors from the chosen resistors. Note that these fractional differences are numerically equal to the fractional differences in the measured transverse energies.

We attach representative examples of these plots below.

---

[7]The values were chosen from the following table of resistors where multiplication by a power of ten is implied:

Table of 1% Resistors

10	13.3	17.8	23.7	31.6	42.2	56.2	75
10.2	13.7	18.2	24.3	32.4	43.2	57.6	76.8
10.5	14	18.7	24.9	33.2	44.2	59	78.7
10.7	14.3	19.1	25.5	34	45.3	60.4	80.6
11	14.7	19.6	26.1	34.8	46.4	61.9	82.5
11.3	15	20	26.7	35.7	47.5	63.4	84.5
11.5	15.4	20.5	27.4	36.5	48.7	64.9	86.6
11.8	15.8	21	28	37.4	49.9	66.5	88.7
12.1	16.2	21.5	28.7	38.3	51.1	68.1	90.9
12.4	16.5	22.1	29.4	39.2	52.3	69.8	93.1
12.7	16.9	22.6	30.1	40.2	53.6	71.5	95.3
13	17.4	23.2	30.9	41.2	54.9	73.2	97.6

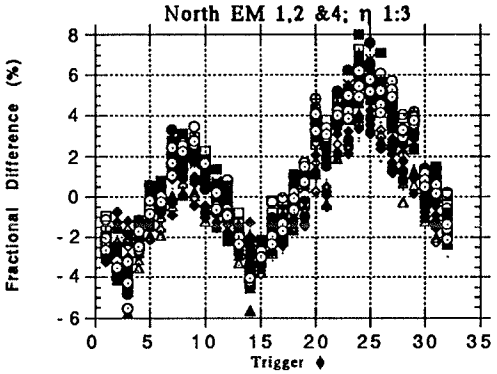

Figure 12a

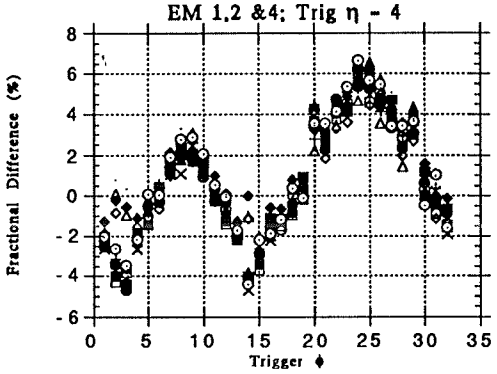

Figure 12b

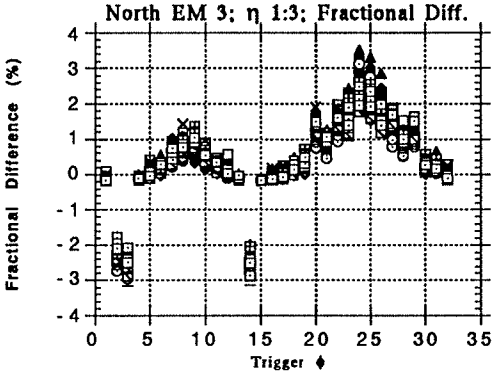

Figure 12c

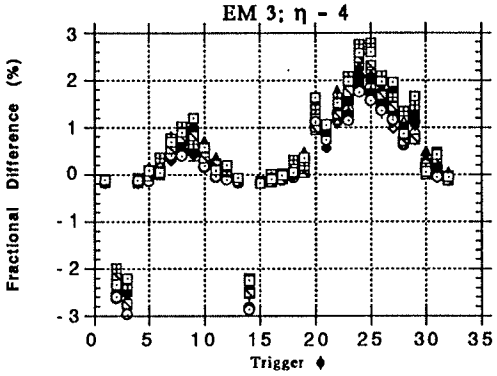

Figure 12d

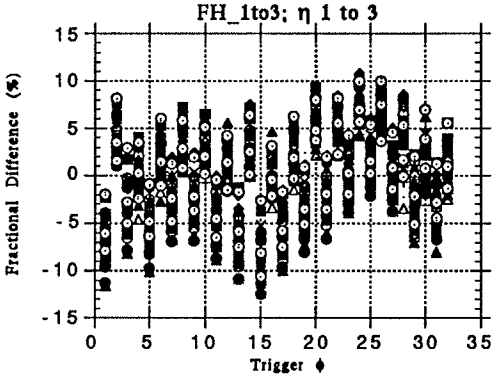

Figure 12e

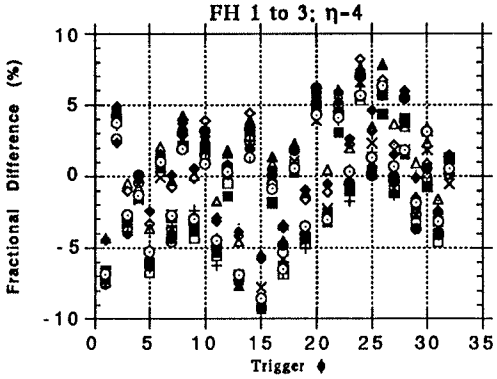

Figure 12f

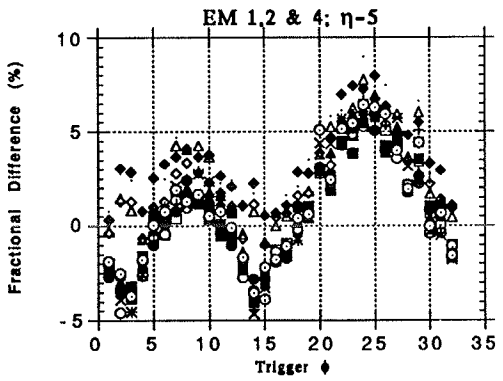

Figure 12g

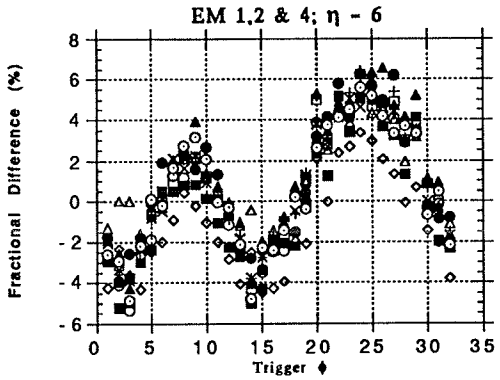

Figure 12h

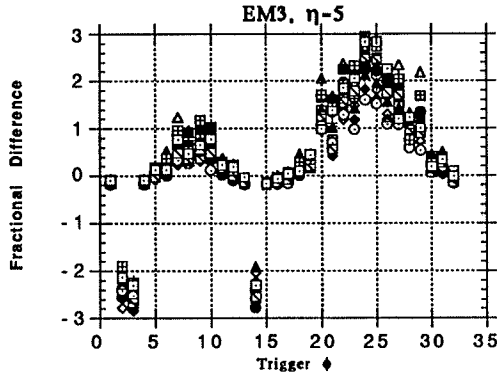

Figure 12i

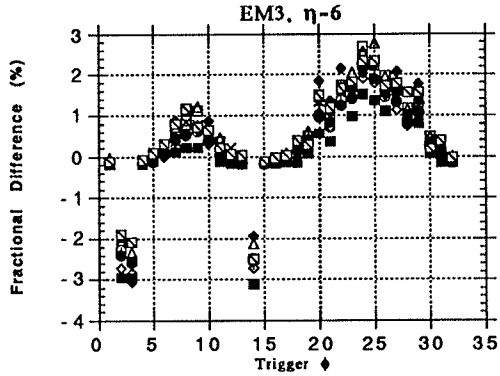

Figure 12j

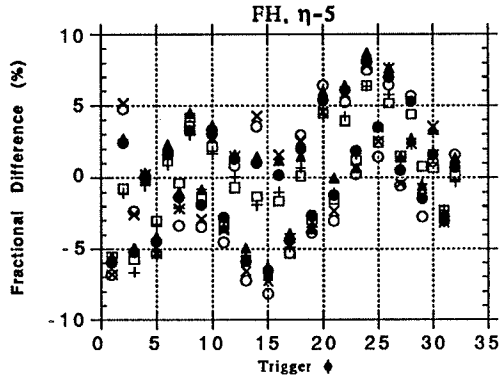

Figure 12k

Note that the FH does not exist for η-6 and also that pieces of the η-5 FH makes no contribution. The lower points for EM3 at ϕ-2,3 and 14 are artefacts of the resistor choice function using two values for the cable length. In any case they are small and will have no effect.

Preferred Solution

Examination of the above plots reveals the fractional discrepancies are in the range of ±5% for the EM sections to ±10% for the HD with a systematic contribution from the cable capacitance variation with ϕ. Elimination of this ϕ dependence would bring the residual scatter of the points to ±2% and ±4% for the EM and HD sections respectively.

The list of chosen resistors is given in Table II below. The values are grouped under their resistor numbers on the BLS cards with the four sets in sequential rows. Thus the 40 resistors needed to make a type 1 BLS card would be obtained by choosing set 1 from the η1/ϕ1 group followed by the corresponding sets from the η1/ϕ2, η2/ϕ1 and η2/ϕ2 groups.

The absence of a connection is indicated by the letters NC and contribution from the EC is indicated by its section number e.g. MFH1.

Table II
CC BLS Resistors

R No.	η1/φ1	9	10	11	12	13	14	15	16	17	18
		EM 1	EM 2	EM31	EM32	EM33	EM34	EM4	FH1	FH2	FH3
Set	1	649	1180	698	698	698	698	649	412	402	402
	2	649	1180	698	698	698	698	649	383	374	383
	3	649	1180	698	698	698	698	649	365	576	NC
	4	649	1180	698	698	698	698	649	MFH1	NC	NC

R No.	η1/φ2	21	22	23	24	25	26	27	28	29	30
		EM1	EM2	EM31	EM32	EM33	EM34	EM4	FH1	FH2	FH3
Set	1	649	1180	698	698	698	698	649	412	402	402
	2	649	1180	698	698	698	698	649	383	374	383
	3	649	1180	698	698	698	698	649	365	576	NC
	4	649	1180	698	698	698	698	649	MFH1	NC	NC

R No.	η2/φ1	60	61	62	63	64	65	66	67	68	69
		EM1	EM2	EM31	EM32	EM33	EM34	EM4	FH1	FH2	FH3
Set	1	649	1180	698	698	698	698	649	402	402	402
	2	649	1180	698	698	698	698	649	374	365	511
	3	649	1180	698	698	698	698	649	511	NC	NC
	4	649	1180	698	698	MFH1	MFH2	NC	NC	NC	NC

R No.	η2/φ2	72	73	74	75	76	77	78	79	80	81
		EM1	EM2	EM31	EM32	EM33	EM34	EM4	FH1	FH2	FH3
Set	1	649	1180	698	698	698	698	649	402	402	402
	2	649	1180	698	698	698	698	649	374	365	511
	3	649	1180	698	698	698	698	649	511	NC	NC
	4	649	1180	698	698	MFH1	MFH2	NC	NC	NC	NC

Note that resistor locations that are not mentioned, numbers 19, 20, 31, 32, 70, 71, 82 and 83 should have no resistors inserted.

Second Summing Stage

Here we show the parallel resistances entering stage 1 and the required resistors for amplitude compensation at stage 2, in consecutive rows for the four BLS species. These are summarized in Tables III and IV respectively.

Table III
Parallel Resistance In Stage 1 Sums

EMS1	HDS1	EMS2	HDS2
51.8	67.5	51.8	67
51.8	63.3	51.8	67.8
51.8	111.7	51.8	255.5
51.8	EC	95.2	EC

Table IV
Stage 2 Sum Resistors

R1EMS2	R1HDS2	R2EMS2	R2HDS2
1210	1240	1210	1240
1210	1240	1210	1270
1210	1330	1210	1430
1210	EC	1330	EC

The values in Table IV are calculated using the functional form (10). The parallel resistance of the two resistors in stage 2 and their respective amplitude sags are given in Table V.

Table V
Stage 2 Parallel Resistors and Amplitude Sag

RPAREM2	RPARHD2	EMSAG2	HDSAG2
605.00	620.00	0.98	0.98
605.00	627.41	0.98	0.98
605.00	689.09	0.98	0.98
633.58	EC	0.98	EC

Note that the amplitude loss at stage 2 is only 2% and hence can be ignored.

Other Effects

Relative Timing of EM and HD

In setting up the triggers, the timing can be adjusted on each CTFE card for each channel but not for EM and HD separately. If we choose to set the timing for FADC conversion for the EM channel then the HD will show additional amplitude sag due to being late. This sag is small being less than about 5% for most channels.

Effect of EC

The items labelled as EC in the tables above are contributions from the EC calorimeter and will be entered as they become known.

Conclusions

We propose to construct 4 separate types of BLS cards for the CC and commence running in this manner. Sufficient uncertainties at the $\pm 5\%$ level make it pointless to attempt higher precision calibration without actual cross-calibration with the full readout using real data. Any miscalibrations that apply to the trigger tower (EM or HD) as a whole can be removed by changing resistor packs at the CTFE cards themselves. Thus, for instance, it will be relatively straightforward to remove the most obvious effect, the ϕ dependence.